

A comparative study on Fabry-Perot interferometer and iodine vapor filter for direct-detection Doppler wind measurements with a Cabanne-Mie lidar

Jia Yue⁽¹⁾, Chiao-Yao She⁽¹⁾, John W. Hair⁽²⁾, Jin-Jia Guo⁽³⁾, Song-Hua Wu⁽³⁾, Zhao-Ai Yan^{(1),(3)}
and Zhi-Shen Liu⁽³⁾

⁽¹⁾Physics Department, Colorado State University, Fort Collins, CO. 80523, U. S. A.,
Email: jyue@lamar.colostate.edu, joeshe@lamar.colostate.edu

⁽²⁾NASA/Langley Research Center, Hampton, Virginia 23681, U. S. A., Email: j.w.hair@larc.nasa.gov

⁽³⁾Ocean Remote Sensing Institute, Ocean University of China, Qingdao 266003, China.

ABSTRACT

Two techniques for frequency analysis are currently employed by different research groups utilizing direct-detection methods for lidar Doppler wind measurements, the double-edge Fabry-Perot interferometer (FPI) and the iodine vapor filter (IVF). The performances of four methods at various frequencies: (a) a double-edge FPI at 1064 nm (ir-FPI), (b) a double-edge FPI at 355 nm (uv-FPI), (c) a single-edge IVF at 532 nm (se-IVF), (d) a double-edge IVF at 532 nm (de-IVF) are analyzed. How the aerosol mixing ratio R_b , affects the instrument sensitivity, signal-to-noise ratio (S/N) and thus wind measurement uncertainty is discussed. Both uv-FPI and ir-FPI have to be utilized to cover different altitude and various aerosol conditions. On the other hand, the IVF system is able to operate consistently for different atmospheric regions. However, the uncertainty in R_b can cause serious errors in wind measurements for IVF systems, thus we discuss not only the means to incorporate a credible determination of R_b , but also its associated S/N degradation in analysis.

1. INTRODUCTION

Direct-detection (incoherent) Doppler lidar systems, taking advantage of the frequency shift of the return molecular (Cabanne) scattering and/or aerosol (Mie) scattering signal using a spectral analyzer, have demonstrated their ability to retrieve the line-of-sight (LOS) wind signal from the planetary layer to the lower mesosphere. Based on the frequency analyzers, the incoherent lidars are divided into two categories: those using a dual Fabry-Perot interferometer (FPI) and those using the iodine vapor filters (IVF). The FPI method was first demonstrated for wind measurement at 532 nm in 1989 [1]. Since the Free-Spectral-Range (FSR) of a FPI filter transmission can be chosen at will, the FSR can be adjusted for lidar wavelength and the dominance in type of scattering. Korb et al. analyzed the wavelength of 1064 nm with a single FPI [2], and later with a dual FPI [3]. A FPI with a larger FSR was employed by Gentry et al. for a 355 nm lidar [4]. Not like the FPI, the working frequency of IVF system is limited by the location of the absorption lines of an iodine filter. The second harmonic Nd:YAG laser at 532 nm can be tuned through several iodine absorption lines. The wind measurements with the single-edge IVF

method were demonstrated independently by two different groups [4] [5], respectively, for aerosol-rich and aerosol-free atmospheres. To extend to the double-edge method, the laser frequency of lidar system is shifted alternately to the midpoints of both edges of the absorption line [6].

The primary goal of this paper is to compare the FPI and IVF techniques of different wavelengths at various atmospheric conditions represented by the aerosol mixing ratio R_b . Two FPIs at 1064 nm and 355 nm are named as ir-FPI and uv-FPI respectively; single-edge and double-edge IVF systems at 532 nm are referred to as se-IVF and de-IVF. Since only molecular Cabanne scattering and aerosol Mie scattering are involved in the scattering processes, we group the above four lidars as Cabanne-Mie lidars. The transmission functions of each frequency analyzer used are illustrated in Fig. 1 with the associated Cabanne-Mie spectra. And their specifications are given in Table 1. Among these, T_{\max} is the maximum value of a filter transmission function (taken to be the same for a unbiased comparison), f_a is the transmission of Mie scattering signal at zero Doppler-shift (zero wind condition), f_m is the transmission of corresponding molecular Cabanne scattering, and ξ is the fraction of scattering signal into each receiving channel.

Based on the system parameters given in Table 1, the fundamental advantages and disadvantages of each method are addressed and compared in this paper. In addition, the method for the determination of R_b , and the impact of R_b measurement on the performance of IVF systems are discussed.

Table 1. Parameters of the 4 frequency analyzer

	FSR (GHz)	$\Delta\nu_{\text{FWHM}}$ (GHz)	T_{\max}	f_a	f_{a2}	f_{m1}	f_{m2}	ξ_1	ξ_2
ir-FPI	3	0.1	0.8	0.4	0.4	0.08	0.08	0.5	0.5
uv-FPI	12	1.7	0.8	0.08	0.08	0.18	0.18	0.5	0.5
se-IVF		1.92	~0.8	0.39	1.0	0.40	1.0	0.6	0.4
De-IVF		1.92	~0.8	0.39	0.39	0.40	0.40	0.9	0.9

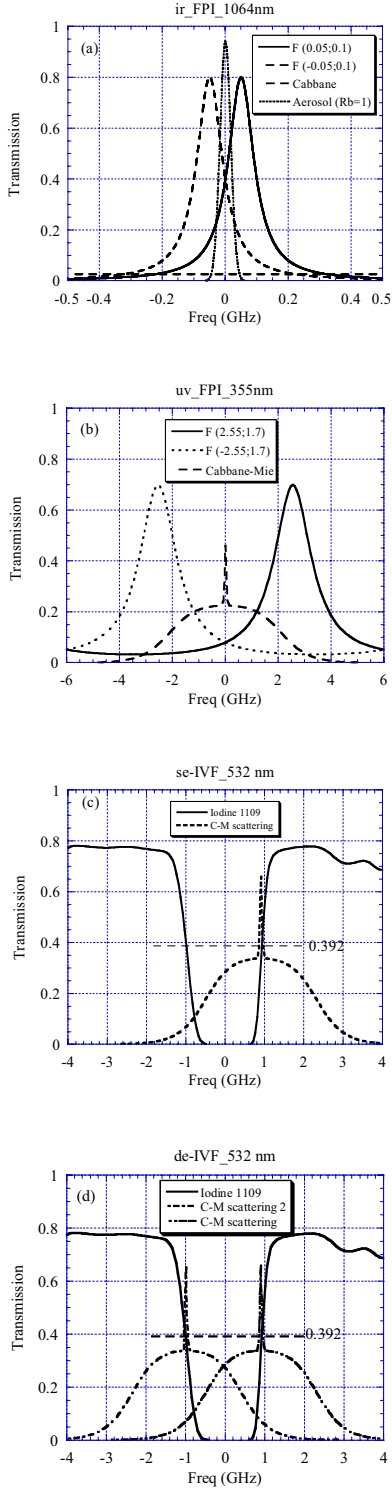


Fig.1. Transmission functions of FPI or IVF with aerosol and Cabanne scattering spectrum.

2. MECHANISM OF FREQUENCY ANALYZERS

For double-edge FPI lidar, the total collected backscattering photons are equally divided into two measurement channels ($\xi = 0.5$). For IVF lidar, in order

to optimize the signal-to-ratio (SNR) and monitor the value of R_b , 10% and 40% of total signal are sent into a reference channel without filters [8], respectively for de-IVF and se-IVF system. The rest of IVF signal is going through a measurement channel with an iodine filter. Since the frequency of de-IVF is tuned alternatively to the midpoints of the two edges of the absorption line, the measurement channel in fact serves as both measurement channels. Assuming unity quantum efficiency for photon-detectors and combining both Mie scattering signal and Cabanne signal, the received photon number for each channel may be expressed as

$$N_{mi} = N \xi_{mi} [R_b f_{ai} + f_{mi}]; \quad i = 1, 2 \quad (1a)$$

$$N_R = N \xi_R [1 + R_b] \quad (1b)$$

Here N is the total received photon number due to Cabanne scattering. The convolution of filter transmission function and aerosol or molecular spectrum respectively, f_a and f_m , are functions of the frequency shift v_D and their zero-shift values are given in Table 1 along with the fractional signals to each channels, ξ_1 and ξ_2 , for either measurement or reference channel ξ_{mi} and ξ_R . The wind ratio $R_W(\Delta v_D, R_b)$, defined as the ratio of two measurement channel signals for double-edge system and the ratio between the measurement and reference channels for single-edge system, depends on the wind-induced Doppler shift, Δv_D , and aerosol mixing ratio, R_b .

$$R_{W-de}(\Delta v_D, R_b) = \frac{N_1}{N_2} = \frac{R_b f_{a1} + f_{m1}}{R_b f_{a2} + f_{m2}} \quad (2a)$$

$$R_{W-se}(\Delta v_D, R_b) = \frac{N_1}{N_2} = \frac{N_m}{N_R} = \frac{\xi_m (R_b f_a + f_m)}{\xi_R (R_b + 1)} \quad (2b)$$

The Doppler frequency shift is then determined by,

$$\Delta v_D = \left(\frac{\Delta R_W}{R_W(0)} \right) / S_{v_D} \quad (3a)$$

$$S_{v_D} = \frac{1}{N_1(0)} \frac{\partial N_1}{\partial v_D} - \frac{1}{N_2(0)} \frac{\partial N_2}{\partial v_D} \quad (3b)$$

With the fractional change of wind ratio, $\Delta R_W/R_W$, observed and the sensitivity S_{v_D} given or a frequency analyzer, the Doppler-shift from laser wavelength, λ , can be calculated, from which the line-of-sight (LOS) wind speed V_{LOS} can be determined by

$$V_{LOS} = -\lambda \Delta v_D / 2 \quad (4)$$

3. COMPARISON OF THE FOUR METHODS

Since the Cabanne-Mie wind lidar we have in mind is a device capable of measuring wind under different aerosol conditions, thus from the planetary boundary layer to the mesosphere, the performance evaluation is carried out as a function of R_b . For a given value of R_b , we calculate the measurement (instrument) sensitivity, and signal-to-noise ratio (SNR) of each system, from which the LOS wind uncertainty is determined. Using Eq. 3b, the measurement sensitivity is calculated at zero Doppler-frequency shift, as is done in general practice. The result is shown in Fig. 2; in the range of stratosphere and lower mesosphere where few aerosols exists ($R_b \approx 0$), the sensitivities are 0, 0.0064, 0.0019 and 0.0038 in $(\text{m/s})^{-1}$ for ir-FPI, uv-FPI, se-IVF and de-IVF respectively. Mainly for lower tropospheric applications, ir-FPI by design is only sensitive to Mie scattering and its associated molecular scattering (relatively weak) contributes only to noise fluctuations. So ir-FPI cannot be used for high altitude wind measurement.

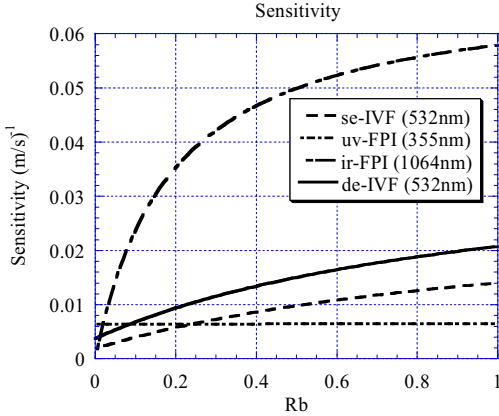


Fig. 2. Sensitivity as a function of aerosol mixing ratio.

For the ease of comparison, we calculate the S/N of each method by assuming a total of 100,000 photons resulting from Cabanne scattering is received, i.e., $N = 100,000$. The variation of the wind ratio, $\delta R_w/R_w$ is due to the photon noise fluctuations (Poisson statistics), which are independent between two channels [8]. Thus the SNR is determined by the detected photons in each channel, including the reference channel. Note that there are only 90,000 photons into the de-IVF measurement channel. Due to the equal duty cycle between two frequencies, the SNR is decreased to $1/\sqrt{2}$ of its single frequency companion. This explains that se-IVF outperforms de-IVF in SNR. SNR of ir-FPI increases dramatically from zero with R_b , while SNR of uv-FPI, being built to minimize the effect of aerosol scattering [9], does not increase that much. In general, se-IVF has the best SNR throughout all regions.

$$SNR = \frac{R_w}{\delta R_w} = \left[\frac{(\delta N_1)^2}{N_1^2} + \frac{(\delta N_2)^2}{N_2^2} \right]^{-\frac{1}{2}} = \left[\frac{1}{N_1} + \frac{1}{N_2} \right]^{-\frac{1}{2}} = \sqrt{\frac{N_1 N_2}{N_1 + N_2}} \quad (5)$$

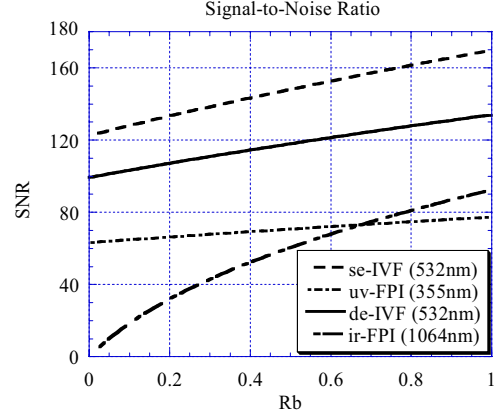


Fig. 3. SNR as a function of aerosol mixing ratio

With the sensitivity S_{V_D} and SNR ratio determined, the LOS wind uncertainty at zero Doppler shift frequency due to photon noise can be calculated with the relation:

$$\delta V_{LOS} = \frac{\lambda \sqrt{(\delta R_w)^2}}{2 R_w S_v} = \frac{1}{S_{V_{LOS}} (SNR)} \quad (6)$$

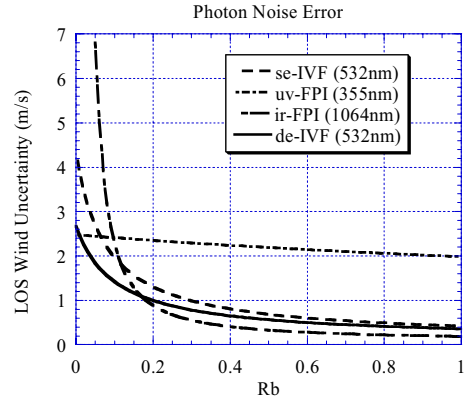


Fig. 4. LOS wind uncertainty as a function of R_b .

As shown in Fig. 4, in an aerosol-free region ($R_b \sim 0$), de-IVF and uv-FPI yield comparative small uncertainties of 2.67 and 2.48 m/s respectively, while se-IVF has higher wind uncertainty of 4.34 m/s because of low sensitivity. The LOS wind uncertainty of ir-FPI decreases from being the highest at aerosol-free region to the lowest among the four methods for $R_b > 0.2$; in contrast, the uncertainty of uv-FPI increases from the lowest to the

largest at high R_b region ($R_b > 0.2$). This indicates that both uv-FPI and ir-FPI need to be utilized to maintain relatively low measurement uncertainty for all R_b conditions. On the other hand, both de-IVF and se-IVF have more consistent performance for all aerosol conditions, using only one IVF system is enough to study various atmospheric regions.

We ignored the comparison in efficiency for photon generation and detection. As discussed in [10], in practice, these differences are likely within a factor of 2.

4. IMPACT OF AEROSOL VARIATION ON IVF METHODS

All the comparisons above are made with the assumption that aerosol mixing ratio R_b s are exactly known. In reality it is not the case, the uncertainty in R_b , δR_b , can introduce extra wind uncertainty represented [10] by

$$\delta V_{LOS} = \frac{\lambda}{2} \frac{\delta R_W}{\delta R_b} \frac{\delta R_b}{R_W S_v} \quad (7)$$

The uv-FPI depends mainly on molecular scattering and was designed to minimize the effect of aerosol scattering and the uncertainty in LOS wind due to δR_b is negligible. Similarly, ir-FPI considers molecule scattering as background noise and its wind ratio R_W is simplified to $f_{a1}(v)/f_{a2}(v)$ which is independent of R_b variation. On the other hand, for IVF systems, the variation in R_b can cause serious errors in wind measurements. As shown in Fig.5, the effect of R_b variation on LOS wind uncertainty depends on wind speed. At low wind condition ($v_D \sim 0$), the effect is less than 0.4% of that under high wind condition ($v \sim 0.1$ GHz, or ~ 50 m/s), when the wind uncertainty for de-IVF due to R_b variation is comparable to that due to photon noise. Under such a condition, δR_b induced wind uncertainty cannot be neglected and the total wind uncertainty is the quadrature sum of the two. Aerosol mixing ratio R_b can be determined by the ratio of a reference channel with no filter and an iodine filter channel with laser frequency tuned to the center of the absorption well [5]. The S/N degradation due to the time required to measure R_b will further increase the wind uncertainty somewhat.

5. CONCLUSION

We have compared performances of 4 wind detection methods. Assuming aerosol mixing ratio is known, one has to use both uv-FPI and ir-FPI to cover different atmosphere conditions while only one IVF system is enough to measure all regions. If the aerosol mixing ratio, R_b , is unknown, the wind uncertainty of IVF may increase by a factor of two under high wind conditions.

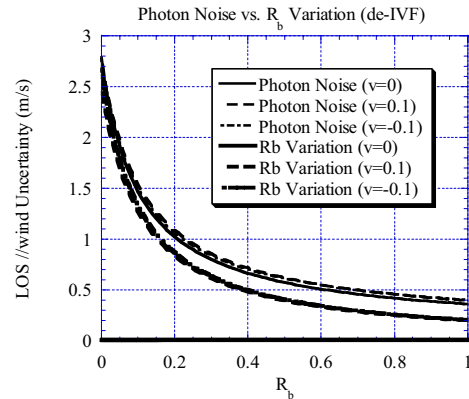


Fig. 5 LOS wind uncertainty due to photon noise and R_b variation under different wind conditions

The work at CSU was supported by US NSF and NASA grants. The work at COU in China was supported by grants from Chinese NSF.

References

1. Chanin M.L., et al., A Doppler lidar for measuring winds in the middle atmosphere, *Geophys. Res. Lett.*, 16, 1273-1276, 1989.
2. Korb C.L., et al., The edge technique: theory and application to the lidar measurement of atmospheric winds, *Appl. Opt.*, 31, 4202-4213, 1992.
3. Korb C.L., et al., Theory of the double-edge technique for Doppler lidar wind measurement, *Appl. Opt.*, 36, 3097-3104, 1998.
4. Gentry B.M., et al., Wind measurements with 355-nm Doppler lidar, *Opt. Lett.*, 25, 1231-1233, 2000.
5. Liu Z.S., et al., Low-altitude atmospheric wind measurement from the combined Mie and Rayleigh backscattering by Doppler lidar with an iodine filter, *Appl. Opt.*, 41, 7079-7086, 2002.
6. Friedman, J.S. et al., Middle-atmospheric Doppler lidar using an iodine-vapor edge filter, *Opt. Lett.*, 22, 1648-1650, 1997.
7. Shibata, Y. et al., Development of two-wavelength Doppler lidar for wind measurement using an iodine edge filter, *20th ILRC*, 85-88, 2000.
8. She, et al., Direct-detection Doppler wind measurement with a Cabanne-Mie lidar: A. Comparison between iodine vapor filter and Fabry-Perot interferometer methods, *Appl. Opt.*, submitted.
9. Garnier, A., and M. L. Chanin, Description of a Doppler Rayleigh LIDAR for measuring winds in the middle atmosphere, *Appl. Phys.*, B 55, 35-40, 1992.
10. She, et al., Direct-detection Doppler wind measurements with a Cabanne-Mie lidar: B. Impact of aerosol variation on iodine vapor filter methods, *Appl. Opt.*, submitted.